Supporting Information

Design of an Air-Cooled Sabatier Reactor for Thermocatalytic Hydrogenation of CO_2: Experimental Proof-of-Concept and Model-Based Feasibility Analysis

Robert Currie, Sogol Mottaghi-Tabar, Yichen Zhuang and David S. A. Simakov*

Department of Chemical Engineering, University of Waterloo, Waterloo ON N2L 3G1, Canada

1. Reaction rate expressions

A Ni/Al_2O_3 catalyst was selected for the reaction (packed bed) compartment. Reaction rate expressions from the literature were implemented, eqs S1-S3.[1] These kinetic expressions, although originally developed for methane steam reforming, account for the reversibility of all reactions involved. Therefore, it is expected that eqs S1-S3 can describe the Sabatier-CO methanation-reverse water gas shift reaction system described by eqs S1-S3. This assumption was experimentally validated using a commercial Ni catalyst (12 wt% Ni/Al_2O_3, BASF, supplied by Research Catalysts, Inc. USA); kinetic parameters were estimated through the non-linear least squares regression.

$$R_1 = \frac{k_1}{p_{H_2}^{2.5}}\left(p_{CH_4}p_{H_2O} - \frac{p_{H_2}^3 p_{CO}}{K_{1,eq}}\right)\frac{1}{\text{den}^2} \tag{S1}$$

$$R_2 = \frac{k_2}{p_{H_2}}\left(p_{CO}p_{H_2O} - \frac{p_{H_2}p_{CO_2}}{K_{2,eq}}\right)\frac{1}{\text{den}^2} \tag{S2}$$

$$R_3 = \frac{k_3}{p_{H_2}^{3.5}}\left(p_{CH_4}p_{H_2O}^2 - \frac{p_{H_2}p_{CO_2}}{K_{3,eq}}\right)\frac{1}{\text{den}^2} \tag{S3}$$

$$\text{den} = 1 + K_{CO}p_{CO} + K_{H_2}p_{H_2} + K_{CH_4}p_{CH_4} + \frac{K_{H_2O}p_{H_2O}}{p_{H_2}}$$

$$k_j = A_j \exp\left(\frac{-E_j}{R_g T}\right) \qquad K_i = B_i \exp\left(\frac{-\Delta H_i}{R_g T}\right) \qquad K_{j,eq} = B_j \exp\left(\frac{-\Delta H_j}{R_g T}\right)$$

2. Estimation of kinetic parameters

To estimate the parameters in eqs S1-S3 (A_j, E_j, B_i and ΔH_i, total 14 parameters), a set of lab experiments were carried out to monitor the change in species concentrations as a function of temperature and space velocity. CO_2 and H_2 were fed by mass flow controllers to a flow reactor containing 0.5g of the catalyst (12 wt% Ni/Al_2O_3, BASF, supplied by Research Catalysts, Inc. USA), with the outlet concentrations monitored using an infrared analyzer (IR-208, Infrared Industries). Parameter estimation was done by minimizing the sum of the squared residuals of the CO_2, CO and CH_4 concentrations by means of the Trust-Region Reflective Algorithm.[2] Simulated mole fractions were obtained by integrating a set of ordinary differential equations (MATLAB ode15s) described by eq S4:

$$\varepsilon \frac{dC_i}{dt} = -\varepsilon v_g \frac{\left(C_i - C_{i,f}\right)}{L} + \rho_c (1-\varepsilon) \sum_j \alpha_i R_{ij} \tag{S4}$$

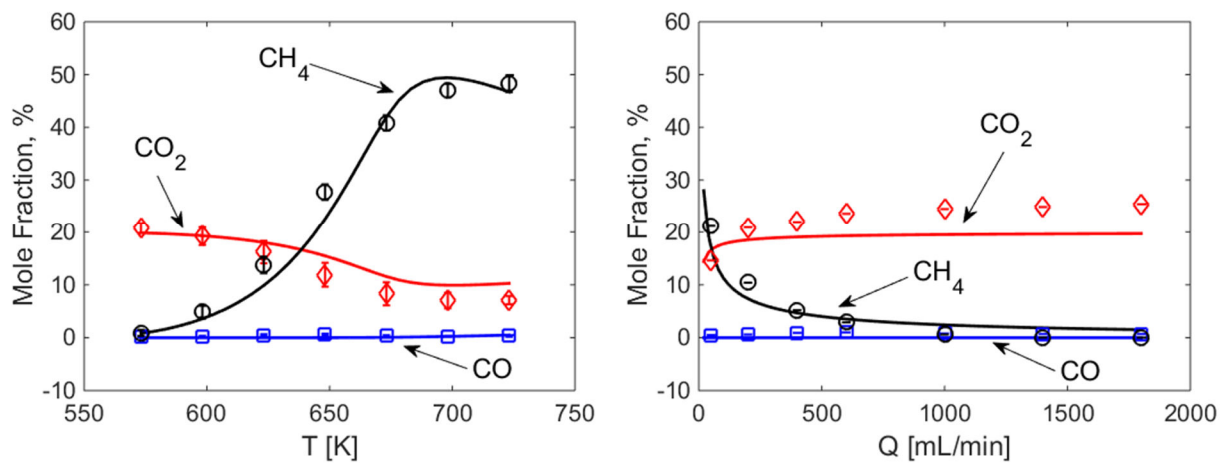

Figure S1. Parameter estimation results, showing the experimentally measured mole fractions (solid lines) and the model prediction (symbols) obtained by integrating eq S4 using the estimated parameters (listed in Table S2).

Equation S4 represents the time evolution of all species participating in the reaction system in a kinetic flow reactor. Initial guesses for the reaction and adsorption constants were adopted from Xu and Froment.[1, 3] The parameter estimation results are shown in Figure S1, with the estimated parameters listed in Table S2. As it can be seen from Figure S1, the adopted rate expressions with the estimated parameters listed in Table S2 satisfactorily predicts the experimentally measured mole fractions of CO_2, CO and CH_4. Note that the parameter estimation predicts that CH_4 formation pathway is reverse water gas shift with subsequent methanation rather than direct methanation of CO_2.

Table S2. Estimated kinetic parameters.

A_1	A_2	A_3	B_{CO}	B_{H_2}	B_{CH_4}	B_{H_2O}
8.90e8	3.42e6	9.22e-5	1.50e-9	1.86e-12	5.48e-7	6.43e3

E_1	E_2	E_3	ΔH_{CO}	ΔH_{H_2}	ΔH_{CH_4}	ΔH_{H_2O}
122.4	93.1	104.8	-97.3	-103.4	-57.7	104.4

Units of activation energies and adsorption enthalpies are kJ/mol. A_1 and A_2 have units of (mol $kPa^{0.5}$)/(kg s). Units of A_2 are mol/(kPa kg s).

3. Transport parameters

Intraparticle and interphase mass and heat transfer limitations were assessed using the following criteria:[4-5]

$$\phi_j^2 = \frac{\hat{k}_j d_p^2}{4D_m} << 1 \tag{S5}$$

$$\frac{\varepsilon\rho_g\left|\Delta H_{RWGS}\right|\hat{k}_j d_p^2}{4k_s T} << \frac{0.75TR_g}{E_a} \tag{S6}$$

$$\frac{\hat{k}_j d_p}{2y_{CO_2,f}k_c} << 0.15 \tag{S7}$$

$$\frac{\varepsilon\rho_g\left|\Delta H_{RWGS}\right|\hat{k}_j d_p}{2h_{gs}T} << \frac{0.75TR_g}{E_a} \tag{S8}$$

$$\hat{k}_1 = \frac{k_1\rho_s(1-\varepsilon)}{\sqrt{P_{tf}}\rho_g\varepsilon} \qquad \hat{k}_2 = \frac{k_2\rho_s(1-\varepsilon)P_{tf}}{\rho_g\varepsilon} \qquad \hat{k}_3 = \frac{k_3\rho_s(1-\varepsilon)}{\sqrt{P_{tf}}\rho_g\varepsilon}$$

In the equations above, k_s is the thermal conductivity of the pellet which was assumed to be the same as for alumina and calculated using an empirical correlation.[6] The gas mass transfer coefficient (k_c) was calculated from the Sherwood number, estimated by the Frossling correlation,[7] eq S9. The effective gas heat transfer coefficient (h_{gs}) was calculated from the Nusselt number, estimated by the analogous correlation for heat transfer,[8] eq S10.

$$Sh = \frac{k_c d_p}{D_m} = 2 + 0.6\,\mathrm{Re}^{0.5}\,\mathrm{Sc}^{\frac{1}{3}} \qquad \mathrm{Re}_p = \frac{v_g\rho_g d_p}{\mu_g} \qquad Sc = \frac{\upsilon}{D_m} \tag{S9}$$

$$Nu_p = \frac{h_{gs}d_p}{k_t} = 2 + 0.6\,\mathrm{Re}^{0.5}\,\mathrm{Pr}^{\frac{1}{3}} \qquad \mathrm{Pr} = \frac{\upsilon}{\alpha_t} \tag{S10}$$

Under relevant conditions (600-800 K, 5-10 bar, gas velocity of 0.04-0.2 m/s), and using previously estimated kinetic parameters, it was shown that interparticle and interphase transport limitations are negligible for methanation reactions. On the other hand, for the reverse water gas shift reaction the intraparticle mass transfer resistance was found to be significant. To account for

that transport limitation the internal effectiveness factor was calculated (for all reactions), using the standard expression for a spherical pellet:[9]

$$\eta_j = \frac{3}{\phi_j}\left(\frac{1}{\tanh\phi_j} - \frac{1}{\phi_j}\right) \qquad \phi_j = \sqrt{\frac{\hat{k}_j d_p^2}{4D_m}} \tag{S11}$$

Axial mass and heat dispersion in a packed bed were accounted for through the following correlations:

$$D_{ae} = \varepsilon\left(\frac{D_m}{\tau_b} + 0.5 d_p v_g\right) \qquad \tau_b = \frac{1}{\varepsilon^{0.5}} \tag{S12}$$

$$k_{ae} = \lambda_g\left(8 + 0.05\,\mathrm{Re}_p^{1.09}\right) \tag{S13}$$

The effective axial mass dispersion coefficient, eq S12, was calculated using a typical correlation adopted from the literature.[10] The expression for the effective axial heat dispersion coefficient, eq S13, was derived from the heat conductivity correlations developed for catalytic fixed beds,[11-12] by plotting k_{ae} vs. $\mathrm{Re_p}$ in the relevant range and least squares fitting.[13]

Wall heat transfer coefficients for heat exchange between the packed bed and cooling tube, eq S14, and heat loss to the environment, eq S15, were calculated by resistances in series. These parameters account for the contribution of the packed bed (h_{wr}), cooling tube or reactor wall (λ_w), molten salt (h_{wc}), insulation layer (λ_{iw}), and natural convection from the external reactor surface (h_{nc}).

$$U_{w,HE} = \left(\frac{1}{h_{wr}} + \frac{d_w}{\lambda_w} + \frac{1}{h_{wc}}\right)^{-1} \tag{S14}$$

$$U_{w,HL} = \left(\frac{1}{h_{wr}} + \frac{d_w}{\lambda_w} + \frac{d_{iw}}{\lambda_{iw}} + \frac{1}{h_{nc}} \right)^{-1} \tag{S15}$$

The effective wall heat transfer coefficient for the reaction compartment (h_{wr}) was estimated using the following correlation:

$$Nu_p = \frac{h_{wr} d_p}{\lambda_g} = 24 + 0.34\,\mathrm{Re}_p^{0.77} \tag{S16}$$

This expression was obtained in the similar way as eq S13, using a complete set of the original correlations[11-12] and least squares fitting.[13] The effective wall heat transfer coefficient for the coolant tube (h_{wc}) was estimated using the following correlations from the literature: [14-16]

$$\mathrm{Re}_c < 2030 \qquad Nu_c = 3.66 + \frac{0.065\,\mathrm{Re}_c\,\mathrm{Pr}_c (D_c / L)}{1 + 0.04[\mathrm{Re}_c\,\mathrm{Pr}_c (D_c / L)]^{2/3}} \tag{S17}$$

$$2030 < \mathrm{Re}_c < 4000 \qquad Nu_c = 0.012(\mathrm{Re}_c^{\,0.87} - 280)\,\mathrm{Pr}_c^{\,0.4} \left[1 + (D_c / L)^{2/3} \right] \tag{S18}$$

$$\mathrm{Re}_c > 4000 \qquad Nu_c = 0.027\,\mathrm{Re}_c^{\,0.8}\,\mathrm{Pr}_c^{\,1/3} \tag{S19}$$

$$Nu_c = \frac{h_{wc} D_c}{\lambda_c} \qquad \mathrm{Re}_c = \frac{v_c \rho_c D_c}{\mu_c} \qquad \mathrm{Pr}_c = \frac{C_{pc} \mu_c}{\lambda_c}$$

The values for the insulation layer (quartz wool) conductivity (λ_{iw}) and natural convection (h_{nc}) were adopted from the literature.[17-18] These contributions were dominant in eq S15 and the wall heat loss coefficient was nearly constant in all simulations: $U_{w,HL} \approx 0.01$ W/(m^2 K).

4. Conversion, selectivity and carbon balance derivation

CO_2 conversion (X_{CO_2}) and CH_4 selectivity (S_{CH_4}) were obtained from the following equations (y_{CO_2}, y_{CO}, and y_{CH_4} are mole fractions on dry basis):

$$X_{CO_2} = \frac{y_{CO} + y_{CH_4} - \beta(y_{CO} + y_{CO_2} + y_{CH_4})}{(1-\beta)(y_{CO} + y_{CO_2} + y_{CH_4})} \tag{S20}$$

$$S_{CH_4} = \frac{y_{CH_4} - \beta(y_{CO} + y_{CO_2} + y_{CH_4})}{y_{CO} + y_{CH_4} - \beta(y_{CO} + y_{CO_2} + y_{CH_4})} \tag{S21}$$

To obtain eqs S20 and S21, CO_2 conversions to CO, eq S22, and to CH_4, eq 23, are first defined:

$$f_1 = \frac{y_{CO}}{(1-\beta)(y_{CO} + y_{CO_2} + y_{CH_4})} \equiv \frac{F_{CO,out}}{F_{CO_2,f}} \tag{S22}$$

$$f_2 = \frac{y_{CH_4} - \beta(y_{CO} + y_{CO_2} + y_{CH_4})}{(1-\beta)(y_{CO} + y_{CO_2} + y_{CH_4})} \equiv \frac{F_{CH_4,gen}}{F_{CO_2,f}} \tag{S23}$$

β is the CH_4 content in the carbon-based feed, as defined in eq S24:

$$\beta = \frac{F_{CH_4,f}}{F_{CH_4,f} + F_{CO_2,f}} = \frac{F_{CH_4,f}}{F_{C,f}} \tag{S24}$$

The total CO_2 conversion and CH_4 selectivity are then obtained as follows:

$$X_{CO_2} = f_1 + f_2 \tag{S25}$$

$$S_{CH_4} = \frac{f_2}{f_1 + f_2} \tag{S26}$$

Carbon balance (CB) is defined as the total rate of carbon fed to the reactor divided by the rate of carbon exiting the reactor:

$$CB = (y_{CO_2} + y_{CO} + y_{CH_4})(1 + \alpha - f_1 - 4f_2 + \gamma)(1-\beta) \tag{S27}$$

In eq S27, the feed H_2:CO_2 ratio (α) and feed CH_4:CO_2 ratio (γ) are defined as follows:

$$\alpha = \frac{F_{H_2,f}}{F_{CO_2,f}} \tag{S28}$$

$$\gamma = \frac{F_{CH_4,f}}{F_{CO_2,f}} \tag{S29}$$

To obtain eq S27, the carbon balance definition, eq S30, is expressed in terms of above-mentioned definitions using the total outlet flow rate $F_{t,out}$ defined by eq S31:

$$CB = \frac{F_{C,out}}{F_{C,f}} = \frac{(y_{CO_2} + y_{CO} + y_{CH_4})F_{t,out}}{F_{CO_2,f} / (1-\beta)} \tag{S30}$$

$$F_{t,out} = F_{CO_2,f} + [F_{H_2,f} - F_{CO,out} - 4(F_{CH_4,out} - F_{CH_4,f})] + F_{CH_4,f} \tag{S31}$$

$F_{CO,out}$ and $F_{CH_4,out}$ in eq S31 correspond to the H_2 consumption in the RWGS and Sabatier reactions.

NOMENCLATURE

$a_{c,HE}$	cooling tube surface-to-volume ratio, m^{-1}
$a_{r,HE}$	cooling tube surface-to-packed volume ratio, m^{-1}
$a_{r,HL}$	reactor surface-to-volume ratio, m^{-1}
A_c	total cross-sectional area of cooling tubes, m^2
A_j	pre-exponential factor of the rate coefficient of reaction *j*, units of k_j
B_j	pre-exponential factor of the adsorption coefficient of species *i*, units of K_j
C_i	molar concentration of species i, mol/m^3
C_t	total molar concentration, mol/m^3
C_{pc}	coolant heat capacity, kJ/(kg K)
C_{pg}	gas heat capacity, kJ/(mol K)
d	wall thickness, m
d_p	catalytic pellet diameter, m
D	diameter, m
D_{ae}	effective axial diffusion coefficient, m^2/s
D_m	gas molecular diffusivity, m^2/s
E_j	activation energy of reaction *j*, kJ/mol
G_c	gravimetric (mass) flow rate of coolant, kg/s
h_{nc}	natural convection heat transfer coefficient, kJ/(m^2 s K)
h_w	effective wall heat transfer coefficient, kJ/(m^2 s K)
ΔH_i	adsorption enthalpy change of species *i*, kJ/mol
k_{ae}	effective axial thermal conductivity, kJ/(m s K)
k_j	rate constant of reaction *j*

K_i	adsorption constant of species *i*, bar^{-1}
$K_{j,eq}$	equilibrium constant of reaction *j*
L	reactor length, m
Nu	Nusselt number
p_i	partial pressure of gaseous species *i*, bar
P_t	reactor pressure, bar
Pr	Prandtl number
P_{tf}	total feed gas pressure, bar
Re	Reynolds number
R_j	rate of reaction *j*, mol/(kg s)
R_g	gas constant, kJ/(mol K)
SV	space velocity, h^{-1}
t	time, s
T	reactor temperature, K
T_c	coolant temperature, K
T_e	environment temperature, K
U_w	overall effective wall heat transfer coefficient, kJ/(m^2 s K)
v_g	gas velocity, m/s
V	compartment volume, m^3
z	reactor length coordinate, m

Greek letters

α_{ij}	stoichiometric coefficient of species *i* in reaction *j*
ε	catalyst bed porosity
ϕ	Thiele modulus
η_j	effectiveness factor of reaction *j*

λ	thermal conductivity, kW/(m K)
μ	viscosity, kg/(m s)
ρ_c	coolant density, kg/m^3
ρ_g	gas molar density, mol/m^3
ρ_s	solid density, kg/m^3
τ_b	catalyst bed tortuosity

Subscripts

air	compressed air
c	coolant
eff	effective
eq	equilibrium
f	feed
g	gas
HE	heat exchange
HL	heat loss
int	initial
nc	natural convection
out	outlet
p	pellet
s	solid
MS	molten salt
r	reactor

Abbreviations

LFG	landfill gas
PtG	power-to-gas
RNG	renewable natural gas
TOS	time-on-stream

References

1. Xu, J. G.; Froment, G. F., Methane Steam Reforming, Methanation and Water-Gas Shift: 1. Intrinsic Kinetics. *AIChE J.* **1989,** *35* (1), 88-96.

2. Wu, S. H.; McAuley, K. B.; Harris, T. J., Selection of Simplified Models: II. Development of a Model Selection Criterion Based on Mean Squared Error. *Can. J. Chem. Eng.* **2011,** *89* (2), 325-336.

3. Elnashaie, S. S. E. H.; Adris, A. M.; Alubaid, A. S.; Soliman, M. A., On the Non-Monotonic Behavior of Methane Steam Reforming Kinetics. *Chem. Eng. Sci.* **1990,** *45* (2), 491-501.

4. Simakov, D. S. A.; Luo, H. Y.; Román-Leshkov, Y., Ultra-low loading Ru/γ-Al_2O_3: A highly active and stable catalyst for low temperature solar thermal reforming of methane. *Appl. Catal. B: Environ.* **2015,** *168-169*, 540-549.

5. Mears, D. E., Tests for Transport Limitations in Experimental Catalytic Reactors. *Ind. Eng. Chem. Process Des. Dev.* **1971,** *10* (4), 541-&.

6. Morrell, R., *Handbook of Properties of Technical & Engineering Ceramics*. Her Majesty's Stationery Office: London, 1985.

7. Frössling, N., Uber die Verdunstung fallender Tropfen. *Gerlands Beitr. Geophys.* **1938,** *52*, 170-216.

8. Ranz, W. E.; Marshall, W. R., Evaporation from Droplets: part I and II. *Chem. Eng. Prog.* **1952,** *48*, 141-173.

9. Froment, G. F.; Bischoff, K. B., *Chemical Reactor Analysis and Design*. Wiley: 1979.

10. Berger, R. J.; Perez-Ramirez, J.; Kapteijn, F.; Moulijn, J. A., Catalyst Performance Testing - Radial and Axial Dispersion Related to Dilution in Fixed-Bed Laboratory Reactors. *Appl. Catal. A-Gen.* **2002,** *227* (1-2), 321-333.

11. Derkx, O. R.; Dixon, A. G., Effect of the Wall Nusselt Number on the Simulation of Catalytic Fixed Bed Reactors. *Catal. Today* **1997,** *35* (4), 435-442.

12. Dixon, A. G.; Cresswell, D. L., Theoretical Prediction of Effective Heat-Transfer Parameters in Packed-Beds. *AIChE J.* **1979,** *25* (4), 663-676.

13. Sun, D.; Simakov, D. S. A., Thermal Management of a Sabatier Reactor for CO_2 Conversion into CH_4: Simulation-Based Analysis. *J. CO_2 Util.* **2017,** *21*, 368-382.

14. Gnielinski, V., New Equations for Heat and Mass-Transfer in Turbulent Pipe and Channel Flow. *Int. Chem. Eng.* **1976,** *16* (2), 359-368.

15. Holman, J. P., *Heat transfer*. 9 ed.; McGraw-Hill: New York, 2002.

16. Mills, A. F., *Heat Transfer*. Irwin: 1992.

17. Sergeev, O. A.; Shashkov, A. G.; Umanskii, A. S., Thermophysical Properties of Quartz Glass. *J. Eng. Phys. Thermophys.* **1982,** *43* (6), 1375-1383.

18. Churchill, S. W.; Chu, H. H. S., Correlating Equations for Laminar and Turbulent Free Convection from a Horizontal Cylinder. *Int. J. Heat Mass Transfer* **1975,** *18* (9), 1049-1053.